The EMBO Journal Vol.16 No.3 pp.659–671, 1997

A small heat shock protein stably binds heat-denatured model substrates and can maintain a substrate in a folding-competent state

Garrett J.Lee[1,2], Alan M.Roseman[3], Helen R.Saibil[3] and Elizabeth Vierling[1]

[1]Department of Biochemistry, The University of Arizona, Tucson, AZ 85721-0106, USA and [3]Department of Crystallography, Birkbeck College, London WC1E 7HX, UK

[2]Corresponding author

The small heat shock proteins (sHSPs) recently have been reported to have molecular chaperone activity *in vitro*; however, the mechanism of this activity is poorly defined. We found that HSP18.1, a dodecameric sHSP from pea, prevented the aggregation of malate dehydrogenase (MDH) and glyceraldehyde-3-phosphate dehydrogenase heated to 45°C. Under conditions in which HSP18.1 prevented aggregation of substrates, size-exclusion chromatography and electron microscopy revealed that denatured substrates coated the HSP18.1 dodecamers to form expanded complexes. SDS–PAGE of isolated complexes demonstrated that each HSP18.1 dodecamer can bind the equivalent of 12 MDH monomers, indicating that HSP18.1 has a large capacity for non-native substrates compared with other known molecular chaperones. Photoincorporation of the hydrophobic probe 1,1′-bi(4-anilino)naphthalene-5,5′-disulfonic acid (bis-ANS) into a conserved C-terminal region of HSP18.1 increased reversibly with increasing temperature, but was blocked by prior binding of MDH, suggesting that bis-ANS incorporates proximal to substrate binding regions and that substrate–HSP18.1 interactions are hydrophobic. We also show that heat-denatured firefly luciferase bound to HSP18.1, in contrast to heat-aggregated luciferase, can be reactivated in the presence of rabbit reticulocyte or wheat germ extracts in an ATP-dependent process. These data support a model in which sHSPs prevent protein aggregation and facilitate substrate refolding in conjunction with other molecular chaperones.

Keywords: heat denaturation/molecular chaperone/protein folding

Introduction

Since exposure to high temperature represents a serious threat to cellular viability, all organisms have developed heat-induced responses that are characterized by the synthesis of highly conserved proteins. In eukaryotes, these proteins include several classes of high molecular weight heat shock proteins (HSPs) as well as the small heat shock proteins (sHSPs) which range in size from 15 to 30 kDa (Lindquist and Craig, 1988). Members of the sHSP family share characteristic C-terminal sequences that have also been conserved in the α-crystallin proteins of the vertebrate eye lens (Plesofsky-Vig *et al.*, 1992; de Jong *et al.*, 1993). Another common feature of sHSPs and α-crystallins is their oligomeric quaternary structure: in the native state they form complexes ranging in size from ~200 to 800 kDa (Vierling, 1991; Arrigo and Landry, 1994). Of the several classes of HSPs, the sHSPs have probably been the least characterized in terms of function.

It is of interest to note that, unlike the high molecular weight HSP90, HSP70 and HSP60 proteins, there is no evidence that sHSPs are essential for normal cellular function. Rather the sHSPs appear to be involved primarily in stress responses and, therefore, may exhibit distinct properties compared with other HSPs. In heat-stressed plants, sHSPs are characteristically abundant and comprise an array of proteins localized to virtually every cellular compartment (Waters *et al.*, 1996). In contrast, mammalian and yeast cells synthesize only a single sHSP which is localized primarily to the cytosol (Arrigo and Landry, 1994).

Several studies have correlated the presence of sHSPs with the acquisition of thermotolerance (Berger and Woodward, 1983; Lin *et al.*, 1984; Rollet *et al.*, 1992; Lavoie *et al.*, 1993; Plesofsky-Vig and Brambl, 1995). While it is not understood mechanistically how sHSPs contribute to the acquisition of thermotolerance, a clearer picture is emerging from both *in vivo* and *in vitro* data. In mammalian systems, the expression of sHSPs has been shown to increase cellular thermoresistance concomitant with the stabilization of cytoskeletal elements such as actin (Lavoie *et al.*, 1993, 1995). Experiments *in vitro* have demonstrated that mammalian sHSPs and α-crystallins can function as molecular chaperones by preventing thermal aggregation of other proteins as well as enhancing their refolding after heat or chemical denaturation (Horwitz, 1992; Jakob *et al.*, 1993; Merck *et al.*, 1993; Buchner, 1996). At minimum, it appears that sHSP-related proteins selectively recognize and stabilize a variety of non-native proteins. Unfortunately, specific information regarding the mechanism of interaction with substrates is lacking and, in the absence of detailed structural information, it remains unclear what structural attributes make sHSPs suited for their observed *in vitro* chaperone activity. However, based on data on the interaction of many different proteins and peptides with molecular chaperones such as GroEL, SecB and HSP70 homologs (reviewed in Hlodan and Hartl, 1994), it is likely that non-native substrates interact with sHSPs through hydrophobic interactions.

We have shown previously that recombinant HSP18.1, a cytosolic class I sHSP from *Pisum sativum* (pea), is a globular, 217 kDa oligomeric protein composed of 12 subunits (Lee *et al.*, 1995). *In vitro*, HSP18.1 also demonstrates functional properties that are consistent with ATP-independent molecular chaperone activity (Lee *et al.*, 1995). For example, when citrate synthase (CS) is dena-

tured at 38°C, stabilization by HSP18.1 leads to increased CS reactivation upon cooling to 22°C. This result implies that CS binding to HSP18.1 at 38°C is transient, or at least can be reversed at lower temperatures. A similar, reversible interaction has been observed at 37°C between mouse HSP25 and CS, in which case CS reactivation was achieved by the addition of oxaloacetic acid, a substrate of CS (Buchner, 1996). However, at higher temperatures such as 45°C, HSP18.1 can suppress the heat-induced aggregation of CS, but cooling does not lead to CS reactivation, suggesting that the interaction between CS and HSP18.1 is no longer reversible. Here, we extend the observation that HSP18.1 protects several different model substrates from thermal aggregation at temperatures above 40°C, and show that under the conditions in which HSP18.1 prevents aggregation, substrates stably bind HSP18.1. In addition, we present evidence that amino acid residues involved in substrate binding are located in a conserved domain of HSP18.1, and that a model substrate stably bound to HSP18.1 is competent for refolding in the presence of mammalian and plant extracts.

Results

HSP18.1 prevents thermal aggregation of malate dehydrogenase and glyceraldehyde-3-phosphate dehydrogenase

We previously showed that HSP18.1 prevented thermal aggregation of CS at 45°C (Lee *et al.*, 1995), but were interested in investigating whether HSP18.1 could confer similar protection to other heat-labile proteins. We chose malate dehydrogenase (MDH), a homodimer, and glyceraldehyde-3-phosphate dehydrogenase (GAPDH), a homotetramer, as model substrates because both proteins were susceptible to heat-induced aggregation at 45°C as measured by light scattering (Figure 1). Although both proteins are dehydrogenases composed of 35 kDa subunits, on the basis of their monomeric concentrations, twice the amount of MDH was required to produce aggregation kinetics similar to those of GAPDH. As previously seen using CS as the substrate, increasing amounts of HSP18.1 prevented heat-induced aggregation of MDH and GAPDH, but suppression of light scattering was not linearly related to HSP18.1 concentration (Figure 1). However, a linear relationship was not expected due to the non-linear concentration dependence of protein aggregation and the size dependence of light scattering (Buchner *et al.*, 1991). Using 100 nM HSP18.1 dodecamer provided complete protection of 300 nM MDH dimer (0.5 MDH subunit:HSP18.1 subunit) from light scattering, and 125 nM HSP18.1 completely protected 75 nM GAPDH tetramer (0.2 GAPDH subunit:HSP18.1 subunit). Previous results showed that 75 nM HSP18.1 completely protected 75 nM CS dimer (0.17 CS subunit:HSP18.1 subunit) from light scattering under similar conditions (Lee *et al.*, 1995). In contrast, the control protein IgG added at the equivalent weight to volume concentration as 100 or 125 nM HSP18.1 only minimally prevented aggregation of MDH or GAPDH.

HSP18.1 stably binds heat-denatured CS, MDH and GAPDH

When HSP18.1 was mixed with either CS, MDH or GAPDH at 22°C, then analyzed by size-exclusion HPLC

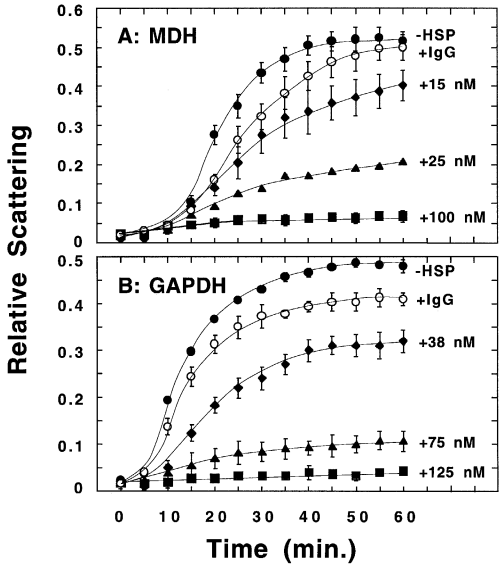

Fig. 1. HSP18.1 prevents thermal aggregation of MDH and GAPDH. In (**A**), 300 nM MDH was incubated at 45°C in the absence or presence of varying concentrations of HSP18.1 or 21 μg/ml bovine IgG (the equivalent weight of 100 nM HSP18.1) as indicated. In (**B**), 75 nM GAPDH was treated similarly to (A) except that IgG was added at a concentration of 27 μg/ml (the equivalent weight of 125 nM HSP18.1). Relative scattering (expressed in arbitrary units) indicative of substrate aggregation was measured as the apparent absorbance at 320 nm. Error bars represent the standard deviation from at least three replicate trials.

(SEC), the proteins eluted with retention times consistent with their native molecular weights (Figure 2). However, when the samples were first heated for various times at 45°C (conditions similar to those in which HSP18.1 prevented thermal aggregation of substrates) then cooled, progressively higher molecular weight species were formed during heating at the expense of native HSP18.1 and substrates (Figure 2). SDS–PAGE of fractions corresponding to each higher molecular weight peak confirmed the presence of both HSP18.1 and the substrates (see Figure 6), demonstrating complex formation. Once formed, complexes were stable for weeks at room temperature and were not affected by treatment with ATP, 0.5 M NaCl or storage at 4°C (not shown). Under similar conditions, no higher molecular weight complexes were formed when bovine IgG was substituted for HSP18.1 (not shown). When HSP18.1 was heated alone for 60 min and analyzed by SEC, no change in retention time or peak area was observed, indicating that HSP18.1 does not change size or become insoluble as a result of heat treatment (Figure 2D). In contrast, samples of CS, MDH or GAPDH heated alone yielded insoluble pellets after centrifugation (not shown), a result consistent with the heat-induced aggregation of these proteins in the absence of HSP18.1. SEC of the corresponding supernatants demonstrated the absence of higher molecular weight peaks and the substantial (or complete for MDH) loss of soluble protein (Figure 2D). Similar pelleting was observed when model substrates were heated in the presence of bovine IgG (not shown). Collectively, these results indicate that HSP18.1 prevents thermal aggregation by selectively binding non-native proteins forming soluble, higher molecular weight complexes.

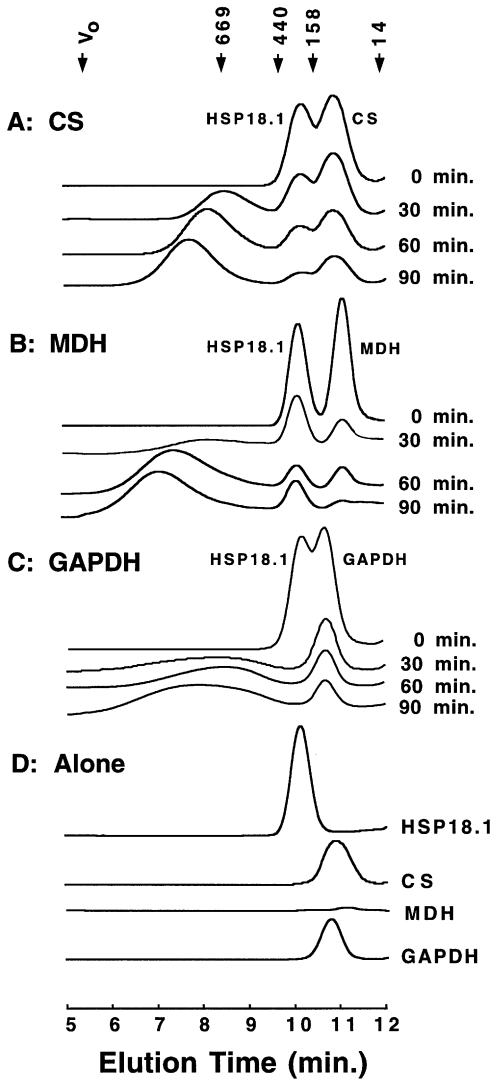

Fig. 2. Heat-denatured substrates form high molecular weight complexes with HSP18.1. HSP18.1 (1 μM) was incubated with 1 μM CS (**A**), 2 μM MDH (**B**) or 1 μM GAPDH (**C**) at 45°C for the indicated times, and then analyzed by SEC as described in Materials and methods. In (**D**), 1 μM HSP18.1, 1 μM CS, 2 μM MDH or 1 μM GAPDH was incubated alone at 45°C for 60 min then similarly analyzed. Proteins were monitored by absorbance at 220 nm. The retention times of protein molecular weight standards are shown above and include blue dextran (2000 kDa) to indicate the void volume.

Temperature dependence of complex formation

To investigate the temperature dependence of complex formation, mixtures of HSP18.1 and the model substrates were heated for 60 min at various temperatures up to 45°C. We have not examined higher temperatures, as temperatures above 45°C are lethal for *P.sativum*, the plant species from which HSP18.1 is derived. For both CS and MDH, higher molecular weight complexes could be detected as shoulders off the HSP18.1 peak after incubation at temperatures as low as 40°C (Figure 3A and B). A similar shoulder indicating complex formation with GAPDH was observed at temperatures as low as 34°C (Figure 3C). In all cases, the apparent size and abundance of complexes increased with increasing temperature, concomitant with the decrease in the amount of free HSP18.1 and substrates.

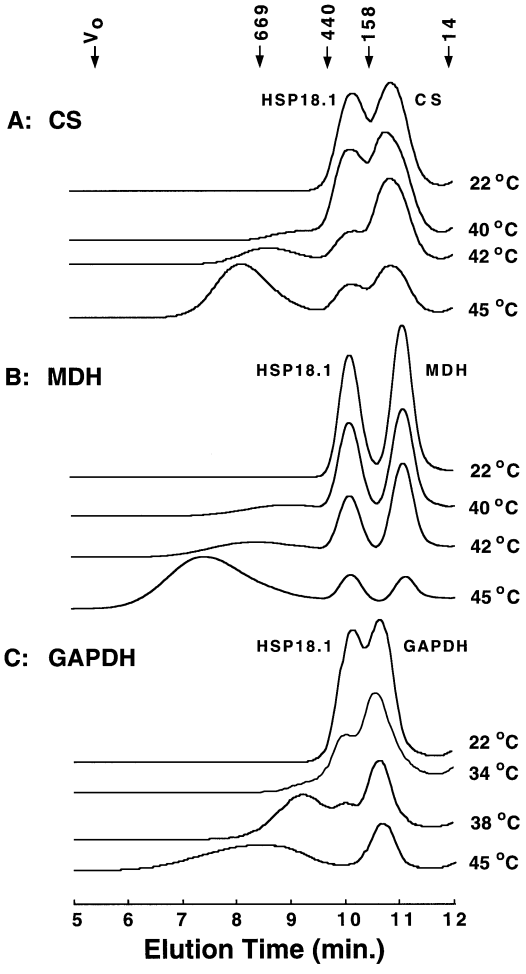

Fig. 3. Temperature dependence of complex formation. HSP18.1 (1 μM) was incubated with 1 μM CS (**A**), 2 μM MDH (**B**) or 1 μM GAPDH (**C**) for 60 min at the indicated temperatures, then analyzed by SEC as described in Materials and methods.

Substrate concentration dependence of complex formation

When 1 μM HSP18.1 dodecamer was incubated with increasing concentrations of substrates for 90 min at 45°C, marked differences in complex formation were observed for each substrate (Figure 4). Since no insoluble material was pelleted during centrifugation of the samples prior to SEC (not shown), presumably all of the original HSP18.1 and substrates remained soluble in either the free or complexed form. For CS, complex formation was already saturated with 1 μM CS dimer (0.17 CS subunit:HSP18.1 subunit) since no difference in retention time or peak area could be detected in the complex formed in the presence of 2 μM CS (Figure 4A).

In the case of MDH, the addition of up to 2 μM MDH dimer (0.33 MDH subunit:HSP18.1 subunit) resulted in the elimination of any free MDH as well as the reduction in, but not the complete elimination of, free HSP18.1 (Figure 4B). However, upon the addition of 3 μM MDH (0.5 MDH subunit:HSP18.1 subunit), essentially no free MDH or HSP18.1 remained. With increasing amounts of MDH up to 3 μM, the apparent molecular weight of the resulting complexes also increased, suggesting that HSP18.1 bound progressively more MDH molecules.

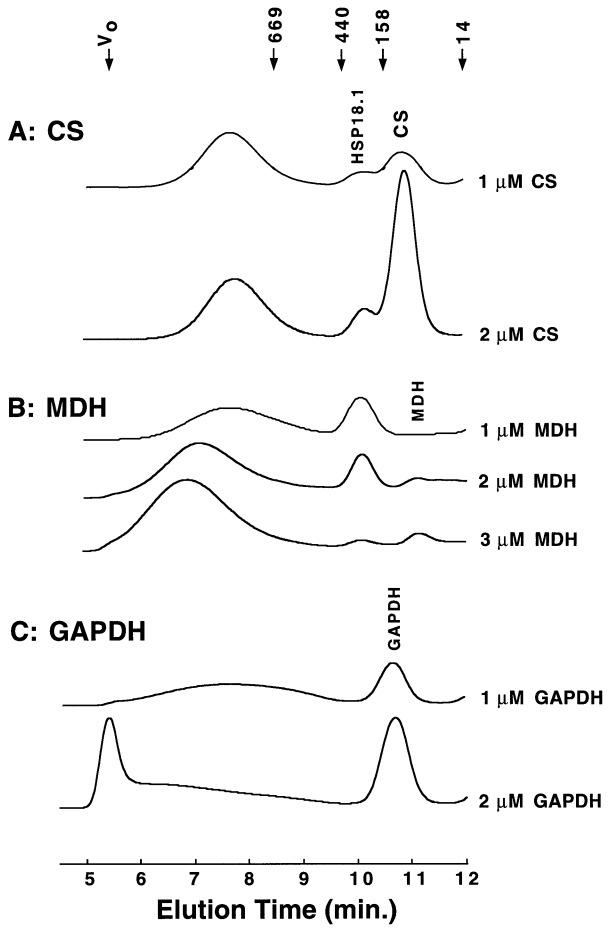

Fig. 4. Substrate concentration dependence of complex formation. HSP18.1 (1 μM) was incubated with the indicated concentrations of CS (**A**), MDH (**B**) or GAPDH (**C**) at 45°C for 90 min, then analyzed by SEC as described in Materials and methods.

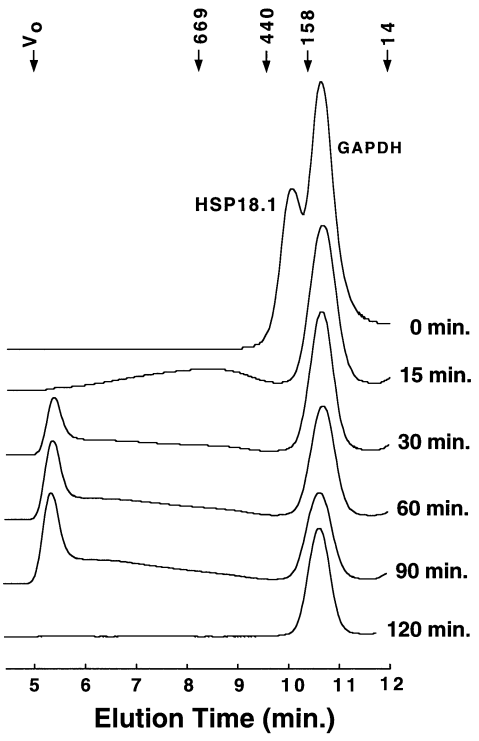

Fig. 5. Time dependence of complex formation in the presence of 2 μM GAPDH. HSP18.1 (1 μM) was incubated with 2 μM GAPDH at 45°C for the indicated times, then analyzed by SEC as described in Materials and methods.

Saturation of the sHSP occurred at ~3 μM MDH because the addition of 4 μM MDH (0.67 MDH subunit:HSP18.1 subunit) did not change the disposition of the complex from that formed in the presence of 3 μM MDH, but did result in the appearance of free, soluble MDH (not shown). The appearance of ~1 μM free MDH suggested that while the majority of MDH aggregation was prevented by irreversible binding to the sHSP, some MDH could remain soluble although denatured.

Incubation of 1 μM GAPDH tetramer with 1 μM HSP18.1 dodecamer (0.33 GAPDH subunit:HSP18.1 subunit) at 45°C for 90 min resulted in the formation of complexes that separated as an extremely broad peak (Figure 4C). In contrast, incubation of 1 μM HSP18.1 with 2 μM GAPDH (0.66 GAPDH subunit:HSP18.1 subunit) resulted in the formation of a species with a very short retention time that eluted approximately with the column void volume (Figure 4C). With 1 μM HSP18.1 and 2 μM GAPDH, investigation of the time dependence of formation for the large species demonstrated its appearance after 30 min and maximum accumulation after 90 min (Figure 5). After 120 min, however, all protein except for residual GAPDH precipitated out of solution, as evidenced by a large, insoluble pellet after centrifugation (not shown) and the absence of all high molecular weight species during SEC (Figure 5). In contrast, samples containing HSP18.1 and CS or MDH remained soluble even after 120 min at 45°C, and no decrease in complex retention time was observed (not shown).

Ratio of substrate:HSP18.1 in complexes

In order to examine the substrate:HSP18.1 ratio within the higher molecular weight complexes, the corresponding protein peaks in Figure 4 were collected from the sizing column and subjected to SDS–PAGE, Coomassie blue staining and densitometry (Figure 6). As a standard, substrate:HSP18.1 staining intensity ratios were determined for equivalent weights of purified HSP18.1, CS, MDH and GAPDH (lanes 2, 8 and 12). The equivalent weight staining ratios were 1.35, 0.78 and 1.13 for CS, MDH and GAPDH, respectively. In order to obtain substrate:HSP18.1 ratios on a weight to weight basis, these values were used to normalize the staining ratios for proteins in isolated complexes and subsequently to derive corresponding substrate subunit:HSP18.1 subunit molar ratios.

The CS:HSP18.1 subunit ratio in the complex peak formed between 1 μM HSP18.1 dodecamer and 1 μM CS dimer (Figure 4, 6.5–9.0 min) was 0.27 (lane 1), and is likely to be the saturating value, since increasing amounts of CS did not increase the apparent molecular weight of complexes (Figure 4). MDH:HSP18.1 subunit ratios were 0.35, 0.58 and 0.90 (Figure 6, lanes 3–5) for the isolated peaks formed with 1, 2 and 3 μM MDH dimers, respectively (Figure 4), demonstrating that HSP18.1 binds increasingly more MDH molecules when they are available. To determine whether the typical broadness of peaks resulted from a population of different molecular weight

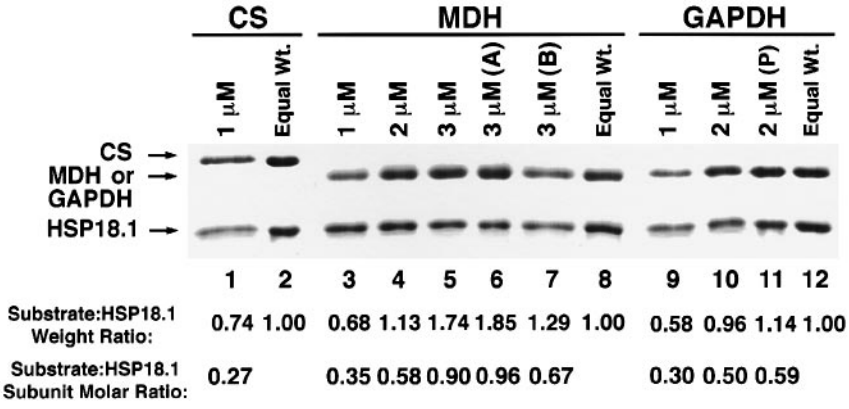

Fig. 6. SDS–PAGE of isolated complexes. HSP18.1 (1 μM) was incubated with various amounts of CS, MDH or GAPDH as indicated, then separated by SEC as shown in Figure 4. HSP18.1–substrate complexes were collected from peaks corresponding to the following minutes in Figure 4: lane 1, 6.5–9.0; lane 3, 6.5–9.9; lane 4, 5.5–8.5; lane 5, 5.0–8.0; lane 6, 5.0–6.75; lane 7, 6.75–8.0; lane 9, 6.0–9.5; lane 10, 5.0–6.0. Fractions were pooled from replicate runs and subjected to SDS–PAGE and Coomassie blue staining. In lane 6, (A) refers to the early eluting half of the entire peak collected and analyzed in lane 5, while in lane 7, (B) refers to the later eluting half. In lane 11, (P) refers to the insoluble pellet formed after 120 min. (Figure 5). In lanes 2, 8 and 12, 'Equal Wt.' refers to samples in which 4 μg of HSP18.1 was mixed with 4 μg of CS, MDH or GAPDH, respectively. For these equal weight mixtures of HSP18.1 with CS, MDH or GAPDH, the substrate to HSP18.1 staining intensity ratios as measured by densitometry were 1.35, 0.78 and 1.13, respectively. 'Substrate: HSP18.1 Weight Ratio' denotes the substrate to HSP18.1 densitometric ratio corrected by the equal weight densitometric ratio.

species as opposed to a population of conformers with a single molecular weight, fractions corresponding to two halves of the peak formed from 3 μM MDH were collected and analyzed. Indeed, the HSP18.1:MDH subunit ratio in the early eluting half was 0.96 (lane 6), while that in the later eluting half was 0.67 (lane 7). This result demonstrates that peaks contain complexes with varying numbers of bound substrate molecules.

Analysis of the broad complex formed between 1 μM HSP18.1 dodecamer and 1 μM GAPDH tetramer (Figure 5) revealed a GAPDH:HSP18.1 subunit ratio of 0.30 (Figure 6, lane 9), while the ratio for the species eluting near the void volume—formed with 2 μM GAPDH (Figure 5)—was 0.50 (Figure 6, lane 10). Interestingly, the insoluble pellet formed after 120 min in the presence of 2 μM GAPDH had a ratio of 0.59 (lane 11), slightly higher than that of the species eluting near the void volume. This finding suggests that the species eluting near the void volume is the precursor of the insoluble species.

Electron microscopy (EM) of HSP18.1 and its MDH complexes

Negative stain EM shows HSP18.1 alone, after heating for 90 min at 45°C and then staining at room temperature, as 8–10 nm diameter particles with layered or angular features (Figure 7A). Similarly sized particles have been observed previously in the absence of heat treatment (Lee *et al.*, 1995), and are consistent with an unaltered 12 subunit oligomeric structure. After heating in the presence of MDH (0.17, 0.34, 0.5 or 1 MDH subunit:HSP18.1 subunit), complexes increased greatly in size, giving a spread of particle diameters between 12 and 40 nm (Figure 7B). There was no marked difference between the size ranges observed for the different MDH:HSP18.1 subunit ratios, although more of the very large particles were observed with a 1:1 subunit ratio. Similar complexes were observed if the sample and negative stain were applied to the grids at 45°C. However, the amount of cooling during the 30 s to 1 min taken to do the staining was not measured.

Conformation of bound MDH

Limited proteinase K digestion was used to determine the global conformation of free or HSP18.1-bound MDH. MDH proved ideal for these studies because conditions could be achieved in which MDH remained entirely in either the free or complexed form. Since incubation of 3 μM MDH dimer with 1 μM HSP18.1 dodecamer for 90 min at 45°C led to quantitative complex formation (Figure 4B), pure complexes could be obtained without chromatographic isolation. When 3 μM MDH was incubated with 1 μM HSP18.1 for 90 min at 22°C [conditions under which MDH remains free (Figure 3B)], then subjected to proteinase K digestion for 10 min on ice, essentially all of the MDH remained resistant up to 100 μg/ml proteinase K (Figure 8). However, when the samples were first heated to 45°C [conditions under which essentially all of the MDH is irreversibly bound to HSP18.1 (Figure 4B)], MDH was hypersensitive to even the lowest proteinase K concentrations (Figure 8). These data are consistent with MDH being bound to HSP18.1 in an unfolded conformation.

Temperature-dependent bis-ANS labeling of HSP18.1

The fluorescent probe 1,1′-bi(4-anilino)naphthalene-5,5′-disulfonic acid (bis-ANS) has been used extensively to demonstrate the presence of hydrophobic sites on the surfaces of proteins. In a recent study, bis-ANS was shown to incorporate covalently into the hydrophobic apical domain of the molecular chaperone GroEL when exposed to UV light (Seale *et al.*, 1995). Using a similar approach, we investigated whether HSP18.1 could be labeled with bis-ANS and, in particular, whether bis-ANS incorporation into HSP18.1 could be increased by incubation at temperatures that favor its stable complex formation with heat-denatured substrates. Indeed, when HSP18.1 was incubated at various temperatures and labeled with bis-ANS, incorporation increased with increasing temperature of incubation (Figure 9A). While labeling of HSP18.1 was only minor at 0°C (Figure 9A, lane 1), moderate labeling

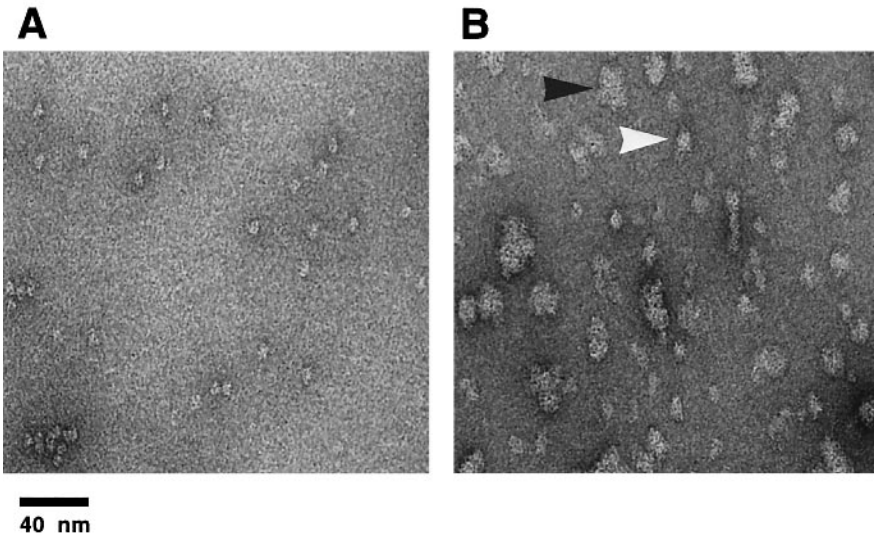

Fig. 7. Negative stain EM image of (**A**) HSP18.1 dodecamers and (**B**) HSP18.1 complexed with unfolded MDH (subunit ratio 0.5 MDH: HSP18.1). The HSP18.1 dodecamers appear as small particles ~8–10 nm in diameter and are seen in a variety of view directions. The complexes with MDH (B) are much larger and less regularly shaped. They range in size from 12 to 40 nm. The white arrow shows a smaller particle, ~10×14 nm, which is consistent with a single dodecamer coated with MDH subunits. A frequently found size is ~16×20 nm. The black arrow shows an example of two particles (each slightly smaller than 16×20 nm) joined together at a seam. The vertical alignment of the particles is caused by the preparation method (see Materials and methods).

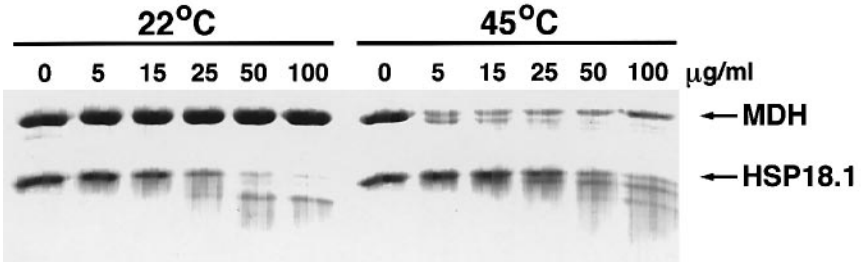

Fig. 8. Bound MDH is proteinase K hypersensitive. HSP18.1 (1 μM) was incubated with 3 μM MDH for 90 min at 22 or 45°C as indicated. Aliquots were subjected to 10 min digestion on ice with the indicated concentrations of proteinase K, then analyzed by SDS–PAGE and Coomassie blue staining.

was observed at 22°C (lane 5). At 38°C or higher, substantial HSP18.1 fluorescence was apparent (lanes 10 and 14). To verify that increased bis-ANS incorporation was not caused simply by temperature-dependent increases in bis-ANS labeling efficiency, IgG was mixed with HSP18.1. At all temperatures evaluated, the heavy chain of IgG was labeled at a relatively low, but uniform level (lanes 2, 7, 11 and 15). To test whether the temperature-dependent increase in HSP18.1 labeling was reversible, HSP18.1 was first heated for 90 min at 45°C, then cooled for 30 min at 22°C. Subsequent bis-ANS labeling of the sHSP at 22°C yielded fluorescence identical to that of a sample that had been incubated and labeled solely at 22°C (lanes 5 and 6). Taken together, these results suggest that HSP18.1 undergoes reversible, temperature-dependent conformational changes that alter surface hydrophobicity.

Bound MDH prevents bis-ANS labeling of HSP18.1

To determine whether the site of bis-ANS incorporation into HSP18.1 is in proximity to the binding sites for heat-denatured substrates, we tested whether binding of heat-denatured MDH to the sHSP blocked subsequent bis-ANS labeling. At 0 or 22°C, essentially no differences in HSP18.1 labeling were observed when 1 μM HSP18.1 dodecamer was incubated and labeled in the presence of either 3 μM MDH dimer or an equivalent weight of IgG (Figure 9A, lanes 2 and 3, and lanes 7 and 8). In contrast, at 38°C, some protection from bis-ANS incorporation could be seen (lanes 11 and 12). Although stable binding of MDH to HSP18.1 was not detected below 40°C by SEC (Figure 2), substantial bis-ANS labeling of MDH at 38°C suggested that, at this temperature, MDH was partially unfolded and may have bound HSP18.1 reversibly, thereby limiting bis-ANS binding. At 45°C in the presence of 3 μM MDH, SEC demonstrated that 1 μM HSP18.1 is saturated with bound MDH (Figure 3). At this temperature and MDH:sHSP ratio, bis-ANS incorporation into the sHSP was almost completely blocked, in contrast to a sample in which an equivalent weight of IgG was substituted for MDH (compare lanes 15 and 16). Coomassie blue staining indicated the presence of equal amounts of HSP18.1, demonstrating that the decrease in HSP18.1 fluorescence in the presence of MDH was not due to aggregation and loss of the sHSP (Figure 9B, lanes 15 and 16). Furthermore, similar levels of protection were also observed when the concentration of bis-ANS was increased to 250 μM, indicating that saturating levels of bis-ANS were present at 100 μM (not shown). These results suggest that bis-ANS photoincorporation into HSP18.1 occurs at or near regions involved in MDH binding.

At 45°C in the presence of HSP18.1, all of the MDH

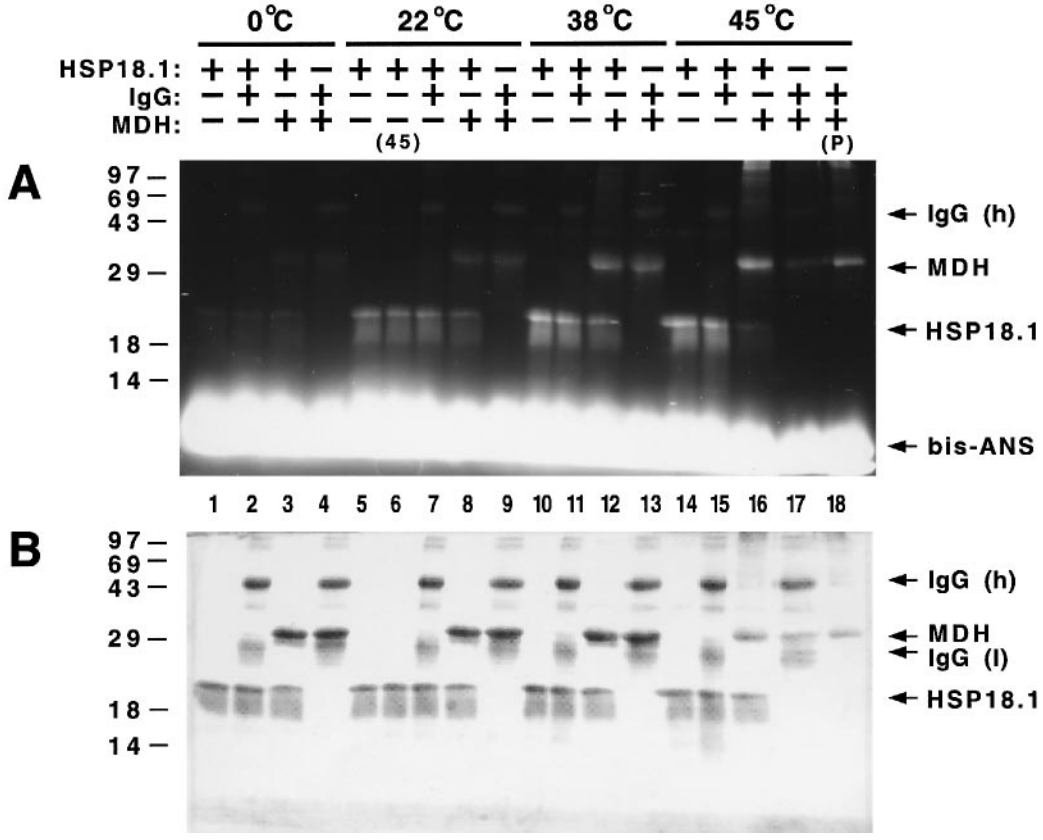

Fig. 9. Bis-ANS labeling. Samples containing 1 μM HSP18.1, 3 μM MDH or 0.22 mg/ml IgG as indicated were incubated for 90 min at the temperatures shown. Samples were irradiated for 20 min with UV light in the presence of 100 μM bis-ANS at the given temperatures, separated by SDS–PAGE then visualized on a UV transilluminator (**A**) or by Coomassie blue staining (**B**). In lane 6, (45) indicates a sample which was first incubated at 45°C for 90 min, then cooled for 30 min at 22°C prior to bis-ANS labeling at 22°C. In lane 18, (P) indicates the pellet fraction formed in the sample. The smearing of the HSP18.1 bands is due to the presence of buffer salts in excess of 100 mM and not proteolysis (G.J.Lee, unpublished observation).

remained in solution and substantial MDH labeling was evident, consistent with the observation that MDH is bound to HSP18.1 in the unfolded state (Figure 8). As expected, nearly all of the MDH heated in the presence of IgG instead of HSP18.1 was found in the insoluble, pellet fraction, but was highly labeled as well (Figure 9A, lane 18). In all MDH-containing samples incubated at 38 or 45°C, several fluorescent, high molecular weight bands were also apparent. Two lines of evidence argue that these high molecular weight species represent MDH molecules cross-linked by the bifunctional molecule bis-ANS: (i) the bands in question formed at the expense of stainable MDH; and (ii) similar high molecular weight species were abundant in the insoluble MDH pellet formed at 45°C (Figure 9A, lane 18).

Localization of incorporated bis-ANS

In order to identify the sites of bis-ANS incorporation into HSP18.1, the sHSP was modified with bis-ANS at 45°C, and cleaved with endoproteinase Arg-C which hydrolyzes peptide bonds on the carboxyl side of Arg residues and, to a lesser extent, Lys residues. Fluorescence measurements of the resulting peptides purified by reverse phase HPLC demonstrated that three peptides, designated A, B and C, were significantly labeled with bis-ANS (Figure 10A). Partial Edman degradation of peptide A revealed the sequence ADLPGLKKEEVKV, which localizes to the highly conserved consensus II region of plant sHSPs (Figure 10B) (Waters, 1995). Peptide A probably extends six more residues to the putative Arg cleavage site at position 84, and would, therefore, encompass the sequence ADLPGLKKEEVKVEVEDDR. Partial sequencing of peptides B and C indicated that the peptides contain redundant sequences that localize to the extreme N-terminus of HSP18.1 (Figure 10). The separation of peptides B and C into two similarly eluting, yet distinct peaks suggest that they represent products of alternative Arg-C cleavage corresponding to the sequences MSLIPSFFSGRR or MSLIPSFFSGR.

Interestingly, reverse phase HPLC did not yield bis-ANS-labeled peptides originating from consensus region I near the C-terminus of the sHSP (Waters, 1995). Consensus region I contains the hydrophobic sequence GVLTVTV of which the GVL motif is essentially invariant among plant sHSPs (Waters, 1995) (Figure 10B). To verify this result, bis-ANS-labeled HSP18.1 was subjected to cyanogen bromide cleavage since the only Met residues in HSP18.1 are within consensus region I (Figure 10B). When the cleavage products were separated by SDS–PAGE on a high resolution peptide gel (Schagger and von Jagow, 1987), then visualized on a UV transilluminator, no fluorescent, low molecular weight bands were detected, despite the presence of a fluorescent, high molecular weight fragment predicted to comprise residues 1–113 (not shown). This finding confirms that bis-ANS modification does not occur in consensus region I.

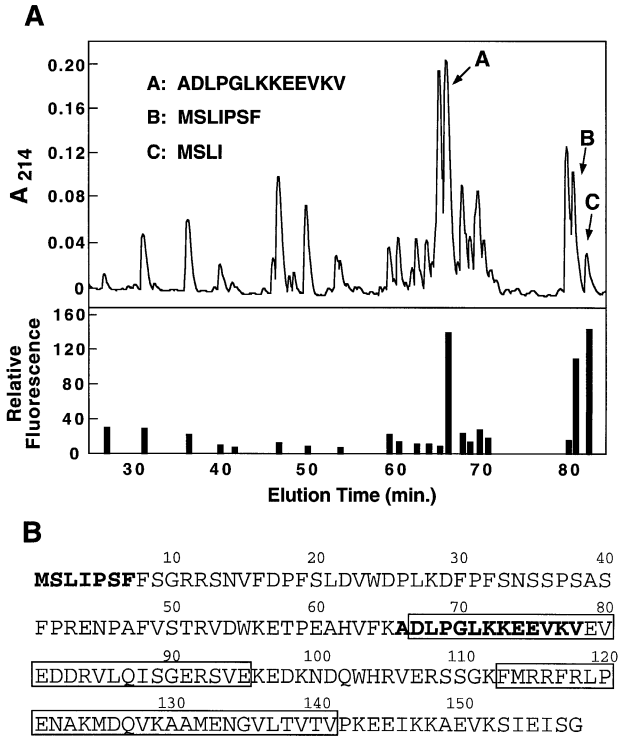

Fig. 10. Separation and identification of bis-ANS-labeled peptides. In (**A**), HSP18.1 was labeled with bis-ANS and digested with endoproteinase Arg-C as described in Materials and methods. The upper panel shows the peptide region of the reverse phase HPLC separation of digestion products, while the lower panel shows the relative fluorescence of isolated peaks. The partial amino-terminal sequences for the bis-ANS-labeled peptides corresponding to peaks A, B and C are shown. In (**B**), the identified sequences (bold) are shown in the context of the entire HSP18.1 sequence. Boxed regions indicate consensus regions II (residues 67–95) and I (residues 113–141) which are highly conserved in all plant sHSPs (Waters, 1995).

Heat-denatured firefly luciferase bound to HSP18.1 is competent for refolding by rabbit reticulocyte lysate and wheat germ extract

We wanted to test whether a heat-denatured substrate bound to HSP18.1 could be refolded in conjunction with other cellular components. To investigate this possibility, we used firefly luciferase, a 61 kDa monomeric protein, as a model substrate because of its absence from most cellular extracts and its highly sensitive activity assay relative to those for CS, MDH and GAPDH. Previous studies have shown that firefly luciferase is a heat-labile protein that aggregates rapidly at 42°C (Schroder *et al.*, 1993). Consistent with this finding, when 1 μM luciferase was heated at 42°C alone or in the presence of 0.2 mg/ml bovine IgG, all of the luciferase formed insoluble aggregates after 15 min (not shown). However, under similar conditions in the presence of 1 μM HSP18.1 dodecamer, luciferase remained soluble but was bound almost exclusively to the HSP in high molecular weight complexes as determined by SEC (Figure 11A). As observed for other model substrates, at 22°C no interaction between native luciferase and HSP18.1 was observed (Figure 11A).

When pre-formed luciferase–HSP18.1 complexes were added to rabbit reticulocyte lysate (RRL), which is a rich source of various molecular chaperones (Frydman *et al.*, 1994), little or no luciferase activity was present immediately after its addition, demonstrating that luciferase was

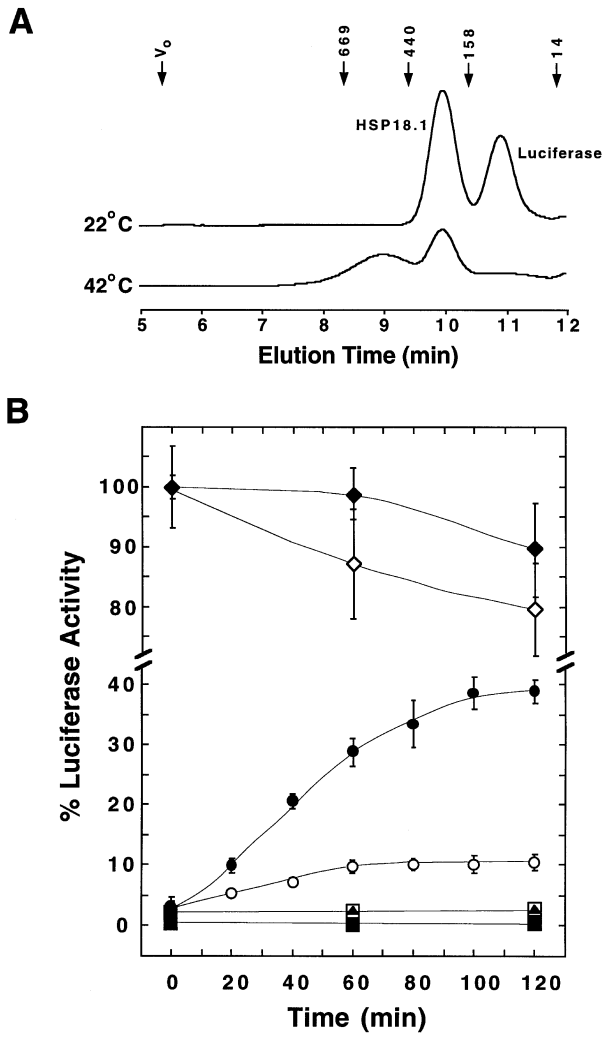

Fig. 11. Heat-denatured luciferase binds to HSP18.1 and is competent for refolding. In (**A**), 1 μM firefly luciferase was incubated with 1 μM HSP18.1 for 15 min at 22 or 42°C, and analyzed by SEC as described in Materials and methods. In (**B**), the following samples were diluted into rabbit reticulocyte lysate (RRL) or wheat germ extract (WGE) supplemented with ATP and measured for luciferase enzymatic activity: unheated mixture of luciferase and HSP18.1 (part A, 22°C) in RRL (◆) or WGE (◇); heated mixture of luciferase and HSP18.1 (part A, 42°C) in RRL (●) or WGE (○); heated mixture of luciferase and bovine IgG in either RRL or WGE (□); and heated mixture of luciferase and HSP18.1 (part A, 42°C) in either RRL or WGE lacking ATP (▲). (■), heated mixture of luciferase and HSP18.1 (part A, 42°C) in buffer supplemented with ATP but lacking RRL or WGE. Error bars represent the standard error from three replicate refolding reactions.

bound to HSP18.1 in an inactive conformation. Over time at 30°C, however, luciferase refolding occurred in a process that was strictly ATP dependent (Figure 11B). Relative to the initial luciferase activity present in an unheated mixture of luciferase and HSP18.1, luciferase reactivation from the pre-formed complexes reached nearly 40% after 2 h, whereas no reactivation occurred if either ATP or RRL was omitted from the refolding reaction. In samples lacking RRL but containing identical buffer components and ATP, SEC revealed that luciferase–HSP18.1 complexes formed at 1 μM luciferase and 1 μM HSP18.1 were completely stable after 2 h at 30°C (not shown). However, the stability of the complexes could

not be determined at the lower concentrations used in the refolding reactions. The folding competency of luciferase bound to HSP18.1 was underscored by the finding that luciferase aggregated by pre-heating in the absence of HSP18.1 remained inactive after addition to reticulocyte lysate and ATP.

To verify that luciferase bound to HSP18.1 was capable of refolding, SEC was used to isolate either bound luciferase (8.5–9.5 min, Figure 11A, 42°C), free luciferase (10.5–11.5 min, Figure 11A, 42°C) or unheated, native luciferase (10.5–11.5 min, Figure 11A, 22°C), and then these fractions were added to ATP-supplemented RRL. Relative to the initial luciferase activity in the native fraction, luciferase activity in the bound fraction increased from 0 to 19%, and from 2 to 5% in the free fraction after 2 h (not shown).

Similar to luciferase refolding observed in RRL, refolding also occurred when pre-formed luciferase–HSP18.1 complexes were added to wheat germ extract (WGE). After 80 min at 30°C in the plant extract, luciferase reactivation reached a maximum of 10% of the initial, native luciferase activity (Figure 11B). As observed in RRL, no luciferase reactivation occurred in WGE if ATP was omitted, or if luciferase had been aggregated in the absence of HSP18.1 prior to its addition into WGE (Figure 11B). Although it is not clear why luciferase reactivation was higher in RRL than in WGE, these results suggest that conserved components within both plant and mammalian systems recognize and assist in the refolding of luciferase bound to HSP18.1.

Discussion

This work demonstrates that, *in vitro*, like many other molecular chaperones, HSP18.1 selectively binds non-native proteins. Complex formation between various heat-denatured proteins and HSP18.1 suggests that stable binding of substrates is the functional basis by which sHSPs prevent thermal aggregation of other proteins. As demonstrated for CS, MDH and GAPDH, the temperature dependence of substrate binding is unique for a given protein and is probably largely determined by a protein's susceptibility to heat denaturation, the exposure of structural elements recognized by HSP18.1, as well as steric considerations. In the case of the model substrate GAPDH, stable complexes with HSP18.1 were formed at temperatures as low as 34°C, which approaches the minimum induction temperature of 30°C for HSP18.1 in pea plants (DeRocher *et al.*, 1991). Thus, the formation of analogous complexes may be predicted to occur *in vivo*.

For the three model substrates CS, MDH and GAPDH, HSP18.1 appears to have the largest binding capacity for heat-denatured MDH. The MDH:HSP18.1 subunit ratios determined for isolated MDH–HSP18.1 complexes revealed that each HSP18.1 subunit can bind up to one MDH monomer. This finding suggests that each HSP18.1 dodecamer can bind up to the equivalent of twelve 35 kDa MDH monomers. However, each substrate polypeptide could potentially contact multiple HSP subunits, and it remains to be determined whether MDH is bound in the monomeric or dimeric form. In comparison with the chaperones GroEL (reviewed in Hlodan and Hartl, 1994) and HSP70 (Palleros *et al.*, 1991) which interact with a single substrate molecule, HSP18.1 appears to have an extremely large substrate binding capacity. Interestingly, both SEC and EM demonstrated that a proportion of the population of HSP18.1 dodecamers could be saturated with the equivalent of 12 MDH monomers even when the concentration of sHSP subunits exceeded the concentration of MDH monomers in the binding reaction. This finding implies that substrate binding is cooperative. For heat-denatured CS, the estimated amount of protein bound to HSP18.1 is lower than that for MDH; the equivalent of up to 0.25 CS subunits may be bound per HSP18.1 subunit. By comparison, HSP16.3, a prokaryotic sHSP from *Mycobacterium tuberculosis*, has been shown recently to bind heat-denatured CS in a ratio of approximately one CS subunit per HSP16.3 subunit. These differences in CS binding capacity may arise from fundamental structural differences between HSP18.1 and HSP16.3. HSP16.3 has been proposed to exist as a trimer of trimers, giving rise to an oligomer with 3-fold symmetry (Chang *et al.*, 1996). Images of the HSP18.1 dodecamers do not reveal an obvious subunit packing symmetry.

The unusually large GAPDH–HSP18.1 complex which forms in the presence of 1 μM HSP18.1 and 2 μM GAPDH is intriguing because of its apparent size, and the higher concentrations of substrate required to drive its formation. While the structure of this large complex is unknown, SDS–PAGE shows that this species contains six GAPDH monomers per HSP18.1 dodecamer. Formation of this complex at the expense of smaller GAPDH–HSP18.1 complexes and its unusually large apparent molecular weight suggest that several GAPDH–HSP18.1 complexes are associated with one another. Such a large size and/or increasing hydrophobicity may explain its transition to the insoluble fraction after >90 min at 45°C. The insolubility of large GAPDH–HSP18.1 complexes is particularly interesting in light of the observed heat-induced partitioning of soluble, cytoplasmic sHSPs into insoluble and/or structure-bound forms called 'heat shock granules' (Nover *et al.*, 1983). The heat-induced transition of soluble sHSPs into large, rapidly sedimenting complexes appears to be a property common to all sHSPs, including those in plants, *Drosophila* and vertebrates (reviewed in Nover, 1991). While the composition of heat shock granules has not been well defined, work by Nover and colleagues indicates that heat shock granules exceed 1 MDa in size and contain other proteins as well as mRNA (Nover *et al.*, 1983, 1989).

The sHSP-related α-crystallins of the vertebrate eye lens also form stable complexes *in vitro* with heat-denatured proteins such as carbonic anhydrase (Rao *et al.*, 1993), rhodanese (Das *et al.*, 1996) and γ-, β_L- or β_H-crystallin (Wang and Spector, 1994; Raman *et al.*, 1995; Das *et al.*, 1996). In the case of rhodanese bound to α-crystallin, tryptophan fluorescence suggests that rhodanese is non-native, but considerably more native in conformation than when bound to GroEL (Das *et al.*, 1996). Similarly to HSP18.1 heated in the presence of MDH, it has been estimated that α-crystallin may bind the equivalent of one γ- or β_L-crystallin per α-crystallin subunit (Wang and Spector, 1994). In these studies, however, complex formation required much higher temperatures ranging from 58 to 65°C. Like HSP18.1 heated in the presence of excess GAPDH, insoluble

complexes formed *in vitro* between α-crystallin and γ- or β_L-crystallin when the concentration of soluble, denatured γ or β_L subunits exceeded that of the α subunits (Wang and Spector, 1994).

The proteinase K susceptibility experiments suggest that heat-denatured MDH is bound to the outside of HSP18.1 dodecamers. From EM, the MDH–HSP18.1 complexes in the smaller size range (10×14 nm) are consistent with the HSP18.1 dodecamers coated with heat-denatured MDH. However, the commonest particle dimensions are 16×20 nm. In these cases, 2–4 coated dodecamers (depending on the third dimension of these larger particles, which is not observed) are likely to be cross-linked by MDH. Still larger particles appear to be joined-up pairs of sub-particles (Figure 7B). Since EM images show the same appearances and size distributions of the particles after high temperature staining, it is very unlikely that significant rearrangement of HSP18.1 subunits occurs during heat-induced MDH–HSP18.1 complex formation.

Strong, hydrophobic interactions between denatured proteins and HSP18.1 are the likely basis for the stable binding of substrates to HSP18.1. The substantial increase in bis-ANS labeling of HSP18.1 at temperatures above 22°C suggests that HSP18.1 surface hydrophobicity increases at temperatures that also promote substrate denaturation. Recent studies have shown that α-crystallin binds increasing amounts of the hydrophobic dyes 8-anilino-1-napthalene sulfonate (ANS) (Raman *et al.*, 1995) and bis-ANS (Das and Surewicz, 1995) at temperatures above 30°C, suggesting that α-crystallin also undergoes a temperature-dependent structural change that increases surface hydrophobicity and, potentially, substrate binding. We propose a mechanism in which increased temperature causes conformational changes in both the substrate and sHSP that result in increased surface hydrophobicity, ultimately leading to hydrophobic interactions.

Temperature-dependent structural changes in HSP18.1 most likely prevent premature exposure of hydrophobic binding sites on the sHSP. Such a mechanism may circumvent non-productive interactions with native proteins at lower temperatures. Since HSP18.1 heated alone does not aggregate, the hydrophobic sites may reside within clefts that prevent HSP18.1 self-association. Other molecular chaperones have also developed mechanisms to prevent non-productive hydrophobic interactions. In the case of the chaperonin GroEL, the hydrophobic binding sites for denatured substrates are localized to the apical regions of a central cavity (Braig *et al.*, 1994). For the bacterial chaperone SecB, hydrophobic binding sites are only exposed after an initial interaction between the chaperone and flexible regions of the non-native substrate (Randall, 1992). The lack of substantial HSP18.1 surface hydrophobicity at normal temperatures is consistent with the observation that HSP18.1 interacts reversibly with chemically denatured substrates at 25°C (Lee *et al.*, 1995).

Bis-ANS incorporation within consensus region II of HSP18.1, in conjunction with substrate protection experiments, suggests that consensus II is critical for substrate binding. In HSP18.1 and other plant sHSPs, consensus II contains several highly conserved aliphatic residues with the specific spacing E/D-V/I-K/R-V/I-X-V/I-E-X_3-V/L/I-L/V (Waters, 1995). Such hydrophobic residues may mediate hydrophobic interactions with denatured substrates, while the intervening charged residues may serve to space these residues optimally and aid in hydration of the region. Multiple sequence alignments show that similar, hydrophobic residues are also present in sHSPs and α-crystallins ranging from *Mycobacterium* to mammals (Plesofsky-Vig *et al.*, 1992; de Jong *et al.*, 1993). Aliphatic residues appear to be well suited for interaction with non-native substrates since, in GroEL, several Val and Leu residues have been implicated in substrate binding (Fenton *et al.*, 1994). Although relatively hydrophobic in composition, the extreme N-terminal sequence of HSP18.1 is not highly conserved; similar sequences are found in most, but not all, class I sHSPs (Waters, 1995). From this limited sequence conservation, it is not clear whether residues in this region are actively involved in substrate binding as suggested by bis-ANS labeling. Of particular interest was the finding that bis-ANS did not label consensus region I despite the presence of the hydrophobic sequence GVLTVTV. Although the GVLTV motif is highly conserved in diverse sHSPs and α-crystallins (Plesofsky-Vig *et al.*, 1992; de Jong *et al.*, 1993), exclusion from bis-ANS labeling suggests that this region may be solvent inaccessible and could play a role in the oligomerization of subunits, a property common to all sHSP-related proteins.

Using a partially purified soybean sHSP mixed with total soybean cell extracts, Lin and colleagues (Jinn *et al.*, 1995) recently have demonstrated the presence of immunodetectable sHSPs in higher molecular weight species. The apparent molecular weight increase of the sHSPs occurred at temperatures >37°C, suggesting that sHSPs formed complexes with heat-denatured proteins. Based on this result and those presented here, it is likely that similar sHSP–substrate complexes are formed *in vivo* under physiologically relevant heat stress conditions.

The ATP-dependent ability of plant and mammalian extracts to reactivate luciferase bound to HSP18.1 suggests that other molecular chaperones within these extracts recognize luciferase–HSP18.1 complexes and actively participate in substrate refolding. Since luciferase aggregates were unable to refold in the presence of the extracts, HSP18.1 appears to play a critical role in maintaining the substrate in a folding-competent state. sHSPs may function as a reservoir that maintains heat-denatured proteins in a form from which they can later refold in conjunction with other chaperones. Therefore, the division of labor in the heat shock response could be between sHSPs which prevent rapid protein aggregation through initial binding events, and other molecular chaperones whose primary function is protein refolding. Since refolding of heat-denatured proteins may be extremely slow or impossible at elevated temperatures, sHSPs may provide a store of denatured proteins that can be reactivated upon return to more permissive temperatures.

It remains to be determined what components within RRL and WGE participate in luciferase refolding when bound to HSP18.1. RRL (Frydman *et al.*, 1994; Frydman and Hartl, 1996) and WGE (Kolb *et al.*, 1994) have been shown to possess all the necessary chaperone machinery to fold firefly luciferase from nascent polypeptides and from the chemically denatured state. In RRL, HSP40, HSP70 (HSC70), HSP90 and TRiC have thus far been implicated in luciferase folding (Frydman *et al.*, 1994;

Schumacher *et al.*, 1994; Frydman and Hartl, 1996). Given the conservation of these chaperones and sHSPs in both plant and animal systems (reviewed in Boston *et al.*, 1997), it is likely that homologous chaperone systems act upon luciferase–HSP18.1 complexes in WGE and RRL.

An additional fate of sHSP-bound substrates *in vivo* could potentially involve proteolytic turnover, in which case prevention of aggregation and maintenance of substrates in an unfolded conformation could facilitate their proteolytic processing. Biochemical and genetic data suggest that other molecular chaperones—including the HSP70 and TRiC systems in the eukaryotic cytosol (Frydman and Hartl, 1996) and the DnaK and GroE systems in *Escherichia coli* (reviewed in Parsell and Lindquist, 1993)—are also involved in the turnover of abnormal proteins. Regardless of the subsequent fate(s) of substrates bound to sHSPs, the large binding capacity of HSP18.1 suggests that sHSPs serve as an efficient initial rescue component within heat-stressed cells.

Materials and methods

Materials

Pig heart CS, pig muscle GAPDH, bovine IgG, proteinase K, endoproteinase Arg-C, HEPES and Tris were obtained from Sigma. Pig muscle mitochondrial MDH was obtained from Boehringer Mannheim, and firefly luciferase, RRL and WGE were obtained from Promega Corp. Bis-ANS was obtained from Molecular Probes. Recombinant HSP18.1 was expressed in *E.coli* cells and purified as previously described (Lee *et al.*, 1995).

Protein determination

Protein concentrations were determined with the Bio-Rad protein assay using bovine serum albumin (BSA) as the standard. In the text and figures, the concentration of HSP18.1 refers to the 217 kDa complex composed of 12 subunits, and the concentrations of CS, MDH, GAPDH and luciferase refer to the 100 kDa homodimer, 70 kDa homodimer, 140 kDa homotetramer and 61 kDa monomer, respectively.

Thermal aggregation experiments

MDH (300 nM) or GAPDH (75 nM) were incubated with varying amounts of HSP18.1 in 50 mM sodium phosphate, pH 7.5 (total volume, 1 ml) in covered quartz cuvettes at 25°C. Where indicated, bovine IgG was added as a negative control at the stated concentrations. Samples were incubated in a water bath at 45°C and then monitored for light scattering in a spectrophotometer set at 320 nm as described (Lee *et al.*, 1995). For 300 nM MDH and 75 nM GAPDH alone, absorbance units were 0.052 and 0.050, respectively after 60 min at 45°C.

Formation of HSP18.1–substrate complexes

HSP18.1 (1 μM) was mixed with varying amounts of CS, MDH or GAPDH in 50 mM sodium phosphate, pH 7.5 (200 μl total) in 1.6 ml microfuge tubes. For luciferase–HSP18.1 mixtures, proteins were combined in 0.65 ml tubes (100 μl total) which were pre-treated with 1 mg/ml BSA and washed with H_2O. After incubating the samples for various times at different temperatures, samples were cooled briefly on ice.

Analysis of HSP18.1–substrate complexes

After complexes were formed as described above, samples were centrifuged at 4°C for 15 min at 16 250 *g*, and supernatants were supplemented with 200 mM NaCl. Samples were then analyzed by SEC using a TosoHaas TSK G4000 SW_{XL} column with a mobile phase consisting of 100 mM sodium phosphate (50 mM for luciferase–HSP18.1 mixtures), 200 mM NaCl, pH 7.3, running at 1.0 ml/min at 22°C. Proteins were detected by absorbance at 220 nm.

For the analysis of component proteins within high molecular weight complexes, the corresponding peak fractions were pooled from 8–12 replicate runs, dialyzed against water, and then lyophilized. Samples were resuspended with SDS sample buffer (Laemmli, 1970), separated by SDS–PAGE on 12.5% acrylamide gels and visualized by Coomassie blue staining. Protein bands were quantitated with a Molecular Dynamics Opti-Quant densitometer.

Electron microscopy

HSP18.1 (1 μM) in 25 mM sodium phosphate, pH 7.5 was heated alone or in the presence of 1–3 or 6 μM MDH at 45°C for 90 min, and then cooled on ice and centrifuged at 12 000 *g* for 15 min. The supernatants were negatively stained in 2% uranyl acetate on perforated carbon suppport films and imaged at 40 000× in a JEOL 1200 EX transmission EM operated at 80 kV, at a defocus of 400 nm. The MDH complexes were diluted four times. Images were recorded under low electron dose conditions on regions of stain left in the holes in the carbon film. Although this method can result in some alignment or geometrical distortion due to strain in the unsupported stain layer during drying, it gives better contrast, which is useful for small structures. Estimated particle sizes were based on measurements of ~60 particles each from equivalent areas of complexes made with 1:1 and 1:2 (MDH:HSP18.1) subunit ratios.

Proteinase K susceptibility experiments

HSP18.1 (1 μM) was mixed with 3 μM MDH in 50 mM sodium phosphate, pH 7.5, then incubated for 90 min at either 22 or 45°C. After samples were centrifuged for 15 min at 16 250 *g*, 45 μl aliquots were supplemented with varying amounts of proteinase K and allowed to incubate on ice for 10 min. Reactions were terminated with 5 mM phenylmethylsulfonyl flouride, then separated by SDS–PAGE on 12.5% acrylamide gels followed by Coomassie blue staining.

Bis-ANS labeling

Aliquots of 150 μl containing 1 μM HSP18.1 only, 1 μM HSP18.1 plus 3 μM MDH, 1 μM HSP18.1 plus 0.21 mg/ml bovine IgG (the equivalent weight:volume concentration of 3 μM MDH) or 3 μM MDH plus 0.22 mg/ml bovine IgG (the equivalent weight:volume concentration of 1 μM HSP18.1) in 50 mM phosphate, pH 7.5, were placed in the wells of a 96-well, polystyrene microtiter plate. The wells were covered with parafilm and incubated for 90 min on ice or on heating blocks set at 22, 38 or 45°C. Bis-ANS (100 μM) was added to the samples and the wells were covered with plastic wrap. With continued incubation at the given temperatures, samples were irradiated for 20 min with 254 nm light supplied by a UV light source (Ultra-violet Products Mineralight, 115 V, 60 Hz, 0.16 A) placed 2 cm from the top of the samples. To investigate the effects of heating and cooling on HSP18.1, 1 μM HSP18.1 was first heated for 90 min at 45°C, then incubated in a 22°C water bath for 30 min prior to bis-ANS labeling at 22°C. Following bis-ANS labeling, samples were transfered to microfuge tubes, centrifuged for 15 min at 16 250 *g*, and SDS sample buffer was added to the supernatants. The pellet fraction resulting from the sample containing MDH plus IgG incubated at 45°C was resuspended in SDS sample buffer and brought to a volume equal to that of the soluble samples. Samples were heated for 5 min at 100°C, then subjected to SDS–PAGE on a 12.5% acrylamide gel. Fluorescent bands were photographed on a 340 nm transilluminator, and the gel was later stained with Coomassie blue.

Identification of bis-ANS-labeled peptides

HSP18.1 (5 μM) was labeled with 250 μM bis-ANS at 45°C as described above, and dialyzed at 4°C against 1000 volumes of 100 mM Tris–HCl, pH 8.5 (at 22°C). Approximately 200 μg of labeled HSP18.1 was supplemented with 0.15% SDS, heated at 80°C for 5 min, cooled to room temperature, then digested with 5 μg of endoproteinase Arg-C for 8 h at 37°C. Peptides were separated by reverse phase HPLC on a Rainin Microsorb-MV C_{18} column equilibrated with 0.065% trifluoroacetic acid (TFA) in H_2O. Elution was carried out with a linear gradient of 0% acetonitrile/0.065% TFA in H_2O to 40% acetonitrile/0.058% TFA/60% H_2O at 0.5 ml/min over 90 min. Peak fractions were collected manually. Bis-ANS-labeled peptides were identified by fluorescence on a Perkin-Elmer LS-5B luminescence spectrometer set with excitation and emisson wavelengths of 397 and 496 nm, respectively (Seale *et al.*, 1995). Amino-terminal sequences of bis-ANS-labeled peptides were determined by Edman degradation on an Applied Biosystems 447A sequenator.

Luciferase reactivation experiments

Luciferase (1 μM) was incubated with 1 μM HSP18.1 or 0.21 mg/ml bovine IgG in 50 mM sodium phosphate, pH 7.5 (100 μl total) at 22 or 42°C for 15 min, then cooled to room temperature. To prevent luciferase adsorption to walls, tubes were first treated with 1 mg/ml BSA for 15 min then washed with H_2O. Luciferase was diluted to 25 nM into solutions pre-incubated for 5 min at 30°C containing 30 μl of RRL,

25 mM HEPES (pH 7.5), 5 mM $MgCl_2$, 10 mM KCl, 2 mM dithiothreitol (DTT) and 2 mM ATP (50 µl total), or 30 µl WGE, 25 mM HEPES (pH 7.5), 2.5 mM $MgCl_2$, 2.5 mM $Mg(CH_3CO_2)_2$, 64 mM KCH_3CO_2, 6 mM DTT, 1.4 mM ATP, 12 mM creatine phosphate and 60 µg/ml creatine phosphokinase (50 µl total). For reactions in WGE lacking ATP, samples were supplemented with 0.5 U of potato apyrase; for reactions in RRL lacking ATP, samples were supplemented with apyrase and ATP was omitted. Reactions were incubated at 30°C and, at various times, aliquots were withdrawn, diluted 500-fold into 25 mM HEPES (pH 7.5) and measured for luciferase activity using the Promega luciferase assay system in a Beckman LS 6000IC scintillation counter. The presence of equal amounts of luciferase in various refolding reactions was verified by Western blot analysis using an antibody specific for luciferase (Promega Corp.) (not shown).

Acknowledgements

We thank Wallace Clark of the Arizona Research Laboratories, Division of Biotechnology at the University of Arizona for performing the N-terminal sequence analysis. This research was supported by National Research Initiative Competitive Grants Program award 9302143 from the U.S. Department of Agriculture, Faculty Research Award FRA-420 from the American Cancer Society, National Institutes of Health grant R01-GM42762 (to E.V.) and a National Institutes of Health Postdoctoral Fellowship (to G.J.L).

References

Arrigo,A.-P. and Landry,J. (1994) Expression and function of the low-molecular-weight heat shock proteins. In Morimoto,R., Tissieres,A. and Georgeopoulos,C. (eds), *The Biology of Heat Shock Proteins and Molecular Chaperones*. Cold Spring Harbor Laboratory Press, Cold Spring Harbor, NY, pp. 335–373.

Berger,E.M. and Woodward,M.P. (1983) Small heat shock proteins of *Drosophila* may confer thermal tolerance. *Exp. Cell Res.*, **147**, 437–442.

Boston,R.S., Viitanen,P.V. and Vierling,E. (1997) Molecular chaperones and protein folding in plants. *Plant Mol. Biol.*, **32**, 191–222.

Braig,K., Otwinowski,Z., Hegde,R., Boisvert,D.C., Joachimiak,A., Horwich,A.L. and Sigler,P.B. (1994) The crystal structure of the bacterial chaperonin GroEL at 2.8 Å. *Nature*, **371**, 578–586.

Buchner,J. (1996) Supervising the fold: functional principles of molecular chaperones. *FASEB J.*, **10**, 10–19.

Buchner,J., Schmidt,M., Fuchs,M., Jaenicke,R., Rudolph,R., Schmid,F.X. and Kiefhaber,T. (1991) GroE facilitates refolding of citrate synthase by suppressing aggregation. *Biochemistry*, **30**, 1586–1591.

Chang,A., Primm,T.P., Jakana,J., Lee,I.H., Serysheva,I., Chiu,W., Gilbert,H.F. and Quiocho,F.A. (1996) *Mycobacterium tuberculosis* 16-kDa antigen (Hsp16.3) functions as an oligomeric structure *in vitro* to suppress thermal aggregation. *J. Biol. Chem.*, **271**, 7218–7223.

Das,K.P. and Surewicz,W.K. (1995) Temperature-induced exposure of hydrophobic surfaces and its effect on the chaperone activity of α-crystallin. *FEBS Lett.*, **369**, 321–325.

Das,K.P., Petrash,J.M. and Surewicz,W.K. (1996) Conformational properties of substrate proteins bound to a molecular chaperone α-crystallin. *J. Biol. Chem.*, **271**, 10449–10452.

de Jong,W.W., Leunissan,J.A.M. and Voorter,C.E.M. (1993) Evolution of the α-crystallin/small heat-shock protein family. *Mol. Biol. Evol.*, **10**, 103–126.

DeRocher,A.E., Helm,K.W., Lauzon,L.M. and Vierling,E. (1991) Expression of a conserved family of cytoplasmic low molecular weight heat shock proteins during heat stress and recovery. *Plant Physiol.*, **96**, 1038–1047.

Fenton,W.A., Kashi,Y., Furtak,K. and Horwich,A.L. (1994) Residues in chaperonin GroEL required for polypeptide binding and release. *Nature*, **371**, 614–619.

Frydman,J. and Hartl,F.U. (1996) Principles of chaperone-assisted protein folding: differences between *in vitro* and *in vivo* mechanisms. *Science*, **272**, 1497–1502.

Frydman,J., Nimmesgern,E., Ohtsuka,K. and Hartl,F.U. (1994) Folding of nascent polypeptide chains in a high molecular mass assembly with molecular chaperones. *Nature*, **370**, 111–117.

Hlodan,R. and Hartl,F.U. (1994) How the protein folds in the cell. In Pain,R.H. (ed.), *Mechanisms of Protein Folding*. IRL Press at Oxford University Press, Oxford, pp. 194–228.

Horwitz,J. (1992) α-Crystallin can function as a molecular chaperone. *Proc. Natl Acad. Sci. USA*, **89**, 10449–10453.

Jakob,U., Gaestel,M., Engel,K. and Buchner,J. (1993) Small heat shock proteins are molecular chaperones. *J. Biol. Chem.*, **268**, 1517–1520.

Jinn,T.-L., Chen,Y.-M. and Lin,C.-Y. (1995) Characterization and physiological function of class I low-molecular-mass, heat shock protein complex in soybean. *Plant Physiol.*, **108**, 693–701.

Kolb,V.A., Makeyev,E.V. and Spirin,A.S. (1994) Folding of firefly luciferase during translation in a cell free system. *EMBO J.*, **13**, 3631–3637.

Laemmli,U.K. (1970) Cleavage of structural proteins during the assembly of the head of bacteriophage T4. *Nature*, **227**, 680–686.

Lavoie,J.N., Gingras-Breton,G., Tanguay,R.M. and Landry,J. (1993) Induction of Chinese hamster HSP27 gene expression in mouse cells confers resistance to heat shock. HSP27 stabilization of the microfilament organization. *J. Biol. Chem.*, **268**, 3420–3429.

Lavoie,J.N., Lamert,H., Hickey,E., Weber,L.A. and Landry,J. (1995) Modulation of cellular thermoresistance and actin filament stability accompanies phosphorylation-induced changes in the oligomeric structure of heat shock protein 27. *Mol. Cell. Biol.*, **15**, 505–516.

Lee,G.J., Pokala,N. and Vierling,E. (1995) Structure and *in vitro* molecular chaperone activity of cytosolic small heat shock proteins from pea. *J. Biol. Chem.*, **270**, 10432–10438.

Lin,C.-Y., Roberts,J.K. and Key,J.L. (1984) Acquisition of thermotolerance in soybean seedlings. *Plant Physiol.*, **74**, 152–160.

Lindquist,S. and Craig,E.A. (1988) The heat shock proteins. *Annu. Rev. Genet.*, **22**, 631–677.

Merck,K.B., Groenen,P.J.T.A., Voorter,C.E.M., de Haard-Hoekman, W.A., Horwitz,J., Bloemendal,H. and de Jong,W.W. (1993) Structural and functional similarities of bovine alpha crystallin and mouse small heat-shock proteins. A familiy of chaperones. *J. Biol. Chem.*, **268**, 1046–1052.

Nover,L. (1991) *Heat Shock Response*. CRC Press, Boca Raton, FL.

Nover,L., Scharf,K.-D. and Neumann,D. (1983) Formation of cytoplasmic heat shock granules in tomato cell cultures and leaves. *Mol. Cell. Biol.*, **3**, 1648–1655.

Nover,L., Scharf,K.-D. and Neumann,D. (1989) Cytoplasmic heat shock granules are formed from precursor particles and are associated with a specific set of mRNAs. *Mol. Cell. Biol.*, **9**, 1298–1308.

Palleros,D.R., Welch,W.J. and Fink,A.L. (1991) Interaction of hsp70 with unfolded proteins: effects of temperature and nucleotides on the kinetics of binding. *Proc. Natl Acad. Sci. USA*, **88**, 5719–5723.

Parsell,D.A. and Lindquist,S. (1993) The function of heat-shock proteins in stress tolerance: degradation and reactivation of damaged proteins. *Annu. Rev. Genet.*, **27**, 437–496.

Plesofsky-Vig,N. and Brambl,R. (1995) Disruption of the gene for hsp30, an α-crystallin-related heat shock protein of *Neurospora crassa*, causes defects in thermotolerance. *Proc. Natl Acad. Sci. USA*, **92**, 5032–5036.

Plesofsky-Vig,N., Vig,J. and Brambl,R. (1992) Phylogeny of the α-crystallin-related heat-shock proteins. *J. Mol. Evol.*, **35**, 537–545.

Raman,B., Ramakrishna,T. and Rao,Ch.M. (1995) Temperature dependent chaperone-like activity of alpha-crystallin. *FEBS Lett.*, **365**, 133–136.

Randall,L. (1992) Peptide binding by chaperone SecB: implications for recognition of nonnative stucture. *Science*, **257**, 241–245.

Rao,V., Horwitz,J. and Zigler,J.S. (1993) Alpha crystallin, a molecular chaperone, forms stable complex with carbonic anhydrase upon heat denaturation. *Biochem. Biophys. Res. Commun.*, **190**, 786–793.

Rollet,E., Lavoie,J.N., Landry,J. and Tanguay,R.M. (1992) Expression of *Drosophila*'s 27 kDa heat shock protein into rodent cells confers thermal resistance. *Biochem. Biophys. Res. Commun.*, **185**, 116–120.

Schagger,H. and von Jagow,G. (1987) Tricine-sodium dodecyl sulfate–polyacryamide gel electrophoresis for the separation of proteins in the range from 1 to 100 kDa. *Anal. Biochem.*, **166**, 368–379.

Schroder,H., Langer,T., Hartl,F.-U. and Bukau,B. (1993) DnaK, DnaJ and GrpE form a cellular chaperone machinery capable of repairing heat-induced protein damage. *EMBO J.*, **12**, 4137–4144.

Schumacher,R.J., Hurst,R., Sullivan,W.P., McMahon,N.J., Toft,D.O. and Matts,R.L. (1994) ATP-dependent chaperoning activity of reticulocyte lysate. *J. Biol. Chem.*, **269**, 9493–9499.

Seale,J.W., Martinez,J.L. and Horowitz,P.M. (1995) Photoincorporation of 4,4′-bis(1-anilino-8-naphthalenesulfonic acid) into the apical domain of GroEL: specific information from a nonspecific probe. *Biochemistry*, **34**, 7443–7449.

Vierling,E. (1991) The roles of heat shock proteins in plants. *Annu. Rev. Plant Physiol. Plant Mol. Biol.*, **42**, 579–620.
Wang,K. and Spector,A. (1994) The chaperone activity of bovine α-crystallin. *J. Biol. Chem.*, **269**, 13601–13608.
Waters,E.R. (1995) The molecular evolution of the small heat-shock proteins in plants. *Genetics*, **141**, 785–795.
Waters,E.R., Lee,G.J. and Vierling,E. (1996) Evolution, structure and function of the small heat shock proteins in plants. *J. Exp. Bot.*, **47**, 325–338.

Received on June 26, 1996; revised on October 17, 1996